Colloids and Surfaces B: Biointerfaces 199 (2021) 111551

Contents lists available at ScienceDirect

Colloids and Surfaces B: Biointerfaces

journal homepage: www.elsevier.com/locate/colsurfb

Mixed liposomes containing gram-positive bacteria lipids: Lipoteichoic acid (LTA) induced structural changes

Bhavesh Bharatiya [a], Gang Wang [a], Sarah E. Rogers [b], Jan Skov Pedersen [c], Stephen Mann [d], Wuge H. Briscoe [a,*]

[a] School of Chemistry, University of Bristol, Cantock's Close, Bristol, BS8 1TS, UK
[b] ISIS Neutron and Muon Source, Rutherford Appleton Laboratory, Harwell Oxford, Didcot, OX11 0QX, UK
[c] Department of Chemistry and Interdisciplinary Nanoscience Center (iNANO), Aarhus University, Gustav Wieds Vej 14, Building 1590-252, 8000, Aarhus C, Denmark
[d] Max Planck Bristol Centre for Minimal Biology, Centre for Protolife Research and Centre for Organized Matter Chemistry, School of Chemistry, University of Bristol, Bristol BS8 1TS, UK

ARTICLE INFO

Keywords:
Lipoteichoic acid (LTA)
Gram-positive bacteria membranes
Vesicles
Neutron scattering
Self-Assembly
Mixed liposomes
Bacteria-Mimicking liposomes

ABSTRACT

Lipoteichoic acid (LTA), a surface associated polymer amphiphile tethered directly to the Gram-positive bacterial cytoplasmic membrane, is a key structural and functional membrane component. Its composition in the membrane is regulated by bacteria under different physiological conditions. How such LTA compositional variations modulate the membrane structural stability and integrity is poorly understood. Here, we have investigated structural changes in mixed liposomes mimicking the lipid composition of Gram-positive bacteria membranes, in which the concentration of *Bacillus Subtilis* LTA was varied between 0–15 mol%. Small-angle neutron scattering (SANS) and dynamic light scattering (DLS) measurements indicated formation of mixed unilamellar vesicles, presumably stabilized by the negatively charged LTA polyphosphates. The vesicle size increased with the LTA molar concentration up to ~6.5 mol%, accompanied by a broadened size distribution, and further increasing the LTA concentration led to a decrease in the vesicle size. At 80 °C, SANS analyses showed the formation of larger vesicles with thinner shells. Complementary Cryo-TEM imaging confirmed the vesicle formation and the size increase with LTA addition, as well as the presence of interconnected spherical aggregates of smaller size at higher LTA concentrations. The results are discussed in light of the steric and electrostatic interactions of the bulky LTA molecules with increased chain fluidity at the higher temperature, which affect the molecular packing and interactions, and thus depend on the LTA composition, in the membrane.

1. Introduction

Intermolecular interactions and self-assembly of bacterial lipids at interfaces and in solution are of critical importance to bacterial function in various bacteriological processes, such as colonisation and biofilm formation on different surfaces [1–3]. In addition to phospholipids (Fig. 1]B), e.g. phosphatidylglycerol (PG), phosphatidylethanolamine (PE), and cardiolipin (CL), lipoteichoic acid (LTA) is a key component of Gram-positive bacterial membranes and plays a crucial role in membrane stability [4–6], and it accounts for 1–2 % of the total bacterial cell dry mass [7]. The basic structure of LTA consists of a phosphodiester-linked chain of ~ 25–30 repeating units of glycerolphosphates, also containing about 5−10 mol% glycosyl or D-alanyl ester units [1]. The chain is linked with a glycolipid moiety *via* a phosphodiester bond between the terminal glycerol phosphate unit and the hydroxyl unit of the sugar (cf. Fig. 1B3). LTA is directly tethered to the lipid membrane *via* diacylglycerol and spans over the peptidoglycan layer, which also contains wall attached teichoic acids (WTA) covalently attached to the peptidoglycan layer *via* phosphodiester links with C6 hydroxyl groups of N-acetyl muramic acid sugars (Fig. 1A;B3). Our knowledge of self-assembly and supramolecular structure of LTA both in solution and at interfaces remains limited, which is important to understanding the role of LTA in the sequelae of bacterial infections, inflammation and septic shocks [1,8].

In the *Bacillus subtilis* (*BS*) bacteria membrane, LTA spans most of the thickness of the periplasmic space [9]. The membrane comprises phosphatidylglycerol (PG) as a major phospholipid component along with phosphatidylethanolamine (PE) and cardiolipin (CL) [10]. Other PG

* Corresponding author.
E-mail address: wuge.briscoe@bristol.ac.uk (W.H. Briscoe).

https://doi.org/10.1016/j.colsurfb.2020.111551
Received 25 October 2020; Received in revised form 18 December 2020; Accepted 19 December 2020
Available online 30 December 2020

derivatives, e.g. diglucosyldiacyl glycerol (DGDG), diacylglycerol (DG) and lysylphosphatidylglycerol (L-PG), also contribute to the structural stability and fluidity of the membrane, which could be present in various amounts depending on bacterial growth conditions, e.g. pH, temperature and the presence of enzymes [11].

Mixed liposomes may be formed by the lipids present in the Gram-positive bacteria membrane, which could be used as model systems for studying bacterial membrane structures and interactions. Previous investigations on molecular interactions involving liposomes formed by lipid mixtures comprising PG with cardiolipin indicated the role of charge interactions and lipid chain packing on the bilayer thickness. Liposomes comprising a binary mixture of dipalmitoylphosphatidyl glycerol (DPPG) and tetramyristoyl cardiolipin (TMCL) exhibited a main fluid phase transition temperature minimum at 39.4 °C for the DPPG mole fraction $X_{DPPG} = 0.8$ [12], lower than that of the pure DPPG or TMCL, also resulting in bilayer thickening and lateral inhomogeneity of the charge density. Oszlánczi et al. [13–15] and Arouri et al. [16] reported inhomogeneous domain formation in mixed PG/PE liposomes at specific lipid compositions and disruption of the bilayer and chain packing on addition of sulfadiazine (SD), an antimicrobial peptide. The segregation of lipid domains induced by SD resulted in destabilization due to phase boundary defects. Conversely, the change in the lipid membrane composition could thus be used to alter the SD localization. In another investigation, the pH-dependent thermotropic behaviour of lysyl(L)-DPPG present in *staphylococcus aureus* showed a different phase behaviour compared to parent DPPG with the formation of an interdigitated lamellar phase below its chain melting transition temperature [17]. The hydrolysis of L-DPPG at pH 5 and the presence of lysine as a degradation product resulted in splitting of the main transition temperature peak, which became more pronounced at pH 9.

Very few studies on mixed model membranes containing LTA have been reported. Using differential scanning calorimetry (DSC) measurements, Gutberlet et al. [18] studied the thermotropic phase transitions in the model membrane comprising DPPG and LTA (from *Staphylococcus aureus*). An increase in the main fluid phase transition temperature (T_{main}) and a decrease in the heat capacity (C_p^m) were observe on LTA addition. This was attributed to the long-range interactions between highly charged polyglycerolphosphate chains of LTA and DPPG, providing structural stability to the mixed lipid membrane.

To the best of our knowledge, the interaction of LTA with mixed lipids mimicking the membrane composition of *Bacillus subtilis* has not been reported. The steric and electrostatic interactions between LTA molecules due to its large negatively charged polymer backbone would impose constraints on their packing and interactions. It would also affect their interactions with other lipids, thus affecting membrane segregation behaviour. Here, we report the structure of mixed liposomes containing LTA extracted from *Bacillus subtilis* at different concentrations and different temperatures using small-angle neutron scattering (SANS), complemented by dynamic light scattering (DLS) and Cryo-TEM. Changes in the packing of the membrane lipids and resultant changes in the aggregate size have been observed. The results are interpreted in terms of the enhanced steric confinement and electrostatic repulsion upon LTA addition and the increased fluidity of the mixed lipid-membrane at higher temperatures.

2. Material and methods

The sodium salt of phospholipids, namely dipalmitoyl phosphatidylglycerol (DPPG), dipalmitoyl phosphatidylethanolamine (DPPE) and cardiolipin (CL, C16:0), were purchased from Avanti Polar Lipids, USA. The lipoteichoic acid (LTA) extracted from *Bacillus Subtilis* (*BS*) was purchased from Sigma-Aldrich, UK. The structures of lipids employed

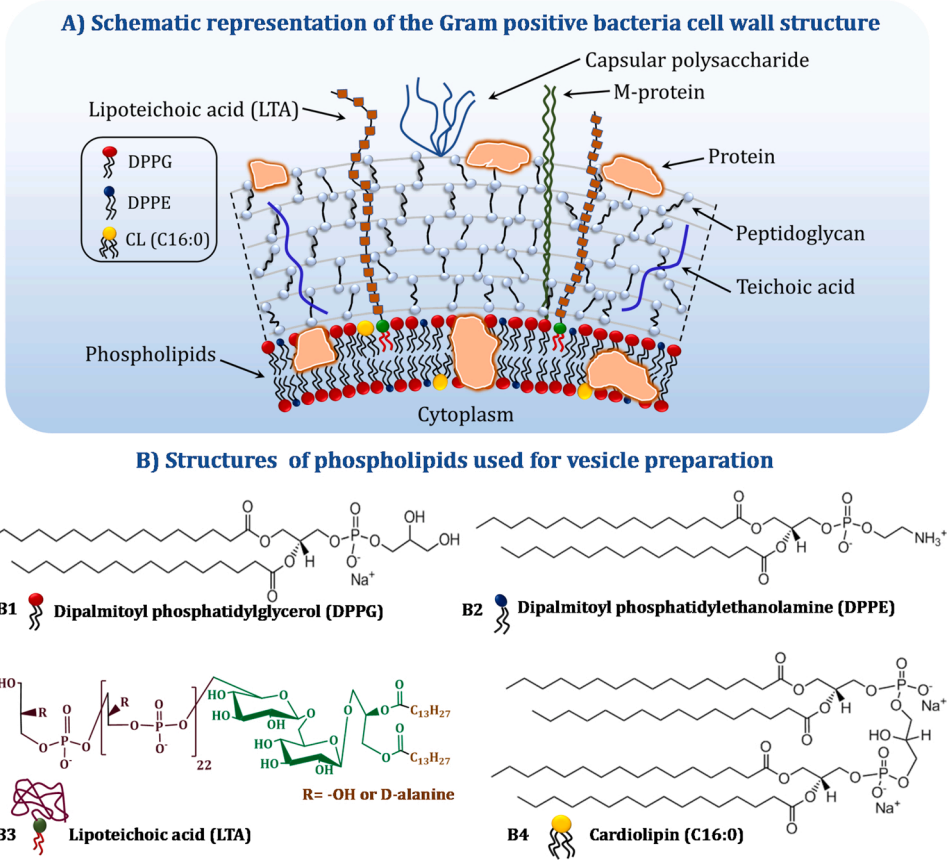

Fig. 1. (A) Structural representation of Gram-positive bacteria cell wall. (B) Structures of lipids used for the preparation of mixed vesicles as model *Bacillus Subtilis* (*BS*) membrane: (B1) DPPG, (B2) DPPE, (B3) *BS* LTA, and (B4) cardiolipin (CL).

for the preparation of mixed vesicles are shown in Fig. 1B. Ultrapure water (resistivity 18.2 MΩ cm and total organic content (ToC) < 4 ppb) used was purified using Millipore® water purification system. Deuterium oxide (D_2O) and organic solvents (chloroform and methanol) used for vesicle preparation were analytical grade reagents purchased from Sigma Aldrich, UK.

2.1. Preparation of mixed lipid vesicles

Designated amounts of DPPG, DPPE and CL (C16:0) were dissolved in a mixture of chloroform and methanol in an 8:2 v/v ratio. The solution was dried in a glass vial under a nitrogen stream and then in a vacuum oven (Heraeus Vacutherm VT 6025) at 30 °C under ~10 mbar for 12 h to obtain a homogeneous lipid thin film. This was followed by hydration using aqueous solutions containing appropriate quantities of LTA for ~ 45 min. For SANS measurements, D_2O was used to prepare the LTA dispersions, while ultrapure water was used for DLS and TEM samples. The mixture was sonicated using a water bath-sonicator at 45 °C for ~ 40 min to obtain an optically transparent dispersion typically containing 1 mg mL^{-1} lipid. This was followed by extrusion in two series, 10 times each through polycarbonate membranes with 200 nm (first series) and 100 nm (second series) pores using a mini extruder (Avanti Polar Lipids, USA). The dispersions were stable for ~ four weeks when stored in fridge at 3–5 °C. Prior to SANS measurements, the sample dispersions were homogenised by sonication at room temperature for 15 min.

2.2. Small-angle neutron scattering (SANS)

SANS measurements were performed on Sans2d small-angle diffractometer at the ISIS Pulsed Neutron Source (STFC Rutherford Appleton Laboratory, Didcot, UK) [19,20], A range of momentum transfer moduli, Q, of 0.0045–0.7 $Å^{-1}$ was achieved by utilizing an incident neutron beam with wavelengths in the range of $\lambda = 1.75$–16.5 Å and employing an instrument setup with both the source-to-sample and the sample-to-detector distance at 4 m, with the 1 m^2 detector offset vertically by 60 mm and sideways 100 mm. Here the momentum transfer is defined as $Q = 4\pi\sin(\theta)/\lambda$, where 2θ is the scattered angle. Each raw scattering data set was corrected for the detector efficiency, sample transmission, and background scattering and converted to scattering cross-section data ($\partial\Sigma/\partial\Omega$ vs Q) using the instrument-specific software [21].

2.3. Dynamic light scattering (DLS)

DLS measurement of the average size of LTA-containing mixed liposomes in water was performed using a Malvern Zetasizer Instrument (Nano-ZS 4800, UK) at a fixed scattering angle of 173° at 25 °C. The incident beam was generated from a He–Ne laser light source with a wavelength of 633 nm. The average values from 3 different measurements, each with 10 runs over 30 s, were reported along with the standard deviation. The hydrodynamic radius (R_h) was obtained using the Stokes-Einstein equation, $D = kT/6\pi\eta R_h$, where k is the Boltzmann constant, T the absolute temperature, D the diffusion coefficient, and η the viscosity of the solvent [22]. Size distributions were obtained by the CONTIN regularized fit option in the Malvern software. Here, the polydispersity index (PDI) is defined as (σ/peak height) [2], where σ is the standard deviation. The measured PDI < 0.05 refers to a perfectly monodisperse sample, while a PDI greater than ~0.7 indicates a very broad size distribution for the measured system.

2.4. Cryogenic-Transmission Electron microscopy (Cryo-TEM)

Cryo-TEM samples were prepared by plunge freezing the sample, using a VITROBOT mark IV FEI, into liquid N_2-cooled liquid ethane. Briefly, droplets (about 4–8 μL) of lipids/LTA dispersions (1 mg mL^{-1}) were placed on glow discharged lacey carbon grids and left for 2 s before blotting (2 s) and plunging. This yielded samples in which liposomes were embedded in vitreous ice suspended inside the holes of the carbon. The sample grid was then transferred into a Gatan 626 cryo-holder and visualised at 200 kV in a Tecnai T20, FEI transmission electron microscope fitted with an Eagle 4k × 4k camera. The images were analysed using the FIJI ImageJ® programme to generate the size histogram of lipid aggregates. All the images were taken using the same operational parameters to allow direct comparison of LTA induced structural changes.

For negative stain TEM, about 4–8 μL of pure LTA or mixed lipid dispersion was deposited on carbon coated 300 mesh size copper grid and incubated for ~5 min. The grids were stained with 2 % (w/v) uranyl acetate and dried for ~15 min. Electron microscopy was performed using a JEOL 1230 transmission electron microscope equipped with a Gatan multiscan digital camera at an accelerating voltage of 80 kV.

2.5. SANS data analysis and calculation of structural parameters

The measured SANS data was analysed in the SASView fitting program, considering the formed structures as vesicles. The shell thickness t and the effective radius r of the spherical vesicles were obtained by fitting the SANS profile, using a *core-shell sphere* (Fig. 2B inset) form factor $P(Q)$ [23],

$$P(Q) = \frac{\phi}{V_s}\left\{\frac{3V_c(\rho_d-\rho_s)J_i(Qr_c)}{Qr_c}+\frac{3V_t(\rho_s-\rho_d)J_i(Qr)}{Qr}\right\}^2 + C \quad (1)$$

where ϕ is the volume fraction of the shell (of thickness t, cf. Fig. 2B), V_s the volume of the shell, V_c the volume of the core, V_t the total volume, r_c the core radius, r the outer shell radius, ρ_d the scattering length density of the solvent D_2O (same as that for the core in this case), ρ_s the scattering length density of the shell, C the background scattering intensity, and the spherical Bessel function $J_i(x) = (\sin x - x\cos x)/x^2$. The scattering intensity was normalized by the volume contributing to the scattering, i.e. the volume of the shell alone, while the SLD of the core was fixed at the same value as that of the solvent. Other models have also been trialled, including the *core-shell ellipsoid model*, which, however, did not describe the SANS data satisfactorily (cf. Section S1 in Supporting Information (SI)).

Although the structure factor is likely not very pronounced due to the dilute LTA concentration (1 mg mL^{-1}), reasonable fits with physically relevant parameters could be achieved by introducing a hard-sphere structure factor $S(Q)$ using the decoupling approximation for moderately polydisperse spherical particles using the Percus-Yevick approximation [24,25]. Here, the interparticle potential is defined as,

$$U(r_d) = \begin{cases} \infty & r_d < 2r \\ 0 & r_d \geq 2r \end{cases} \quad (2)$$

Here, r_d is the distance from the center of a sphere of a radius r.

Given the charged lipid headgroups and the phosphate-containing polymer backbone of LTA, fitting was also attempted using the Hayter-MSA structure factor, but no physically feasible fitting parameters could be achieved. Here, the polydispersity index (PDI) is defined as σ/r for the measured r values within the standard deviation σ.

The SLDs for the mixed lipid systems were calculated based on the available information on the structure of the LTA extracted from *Bacillus Subtilis* [26] and the phospholipids. It is important to note that considerable variations have been reported for the structure and molecular weight (MW) of solvent-extracted LTA. The final molecular formula for LTA assuming 10 mol% D-alanylation is $C_{128}H_{250}O_{130}P_{23}N_5$ (MW = 4649 g mol^{-1}). The calculated SLDs for pure components LTA, DPPG, DPPE and CL (C16:0) are 1.41 × 10^{-6}, 0.385 × 10^{-6}, 0.260 × 10^{-6}, 0.258 × 10^{-6} $Å^{-2}$, respectively. The detailed information on the calculated SLDs for the mixed lipid systems comprising different mol% of LTA is provided in Table S2 in SI.

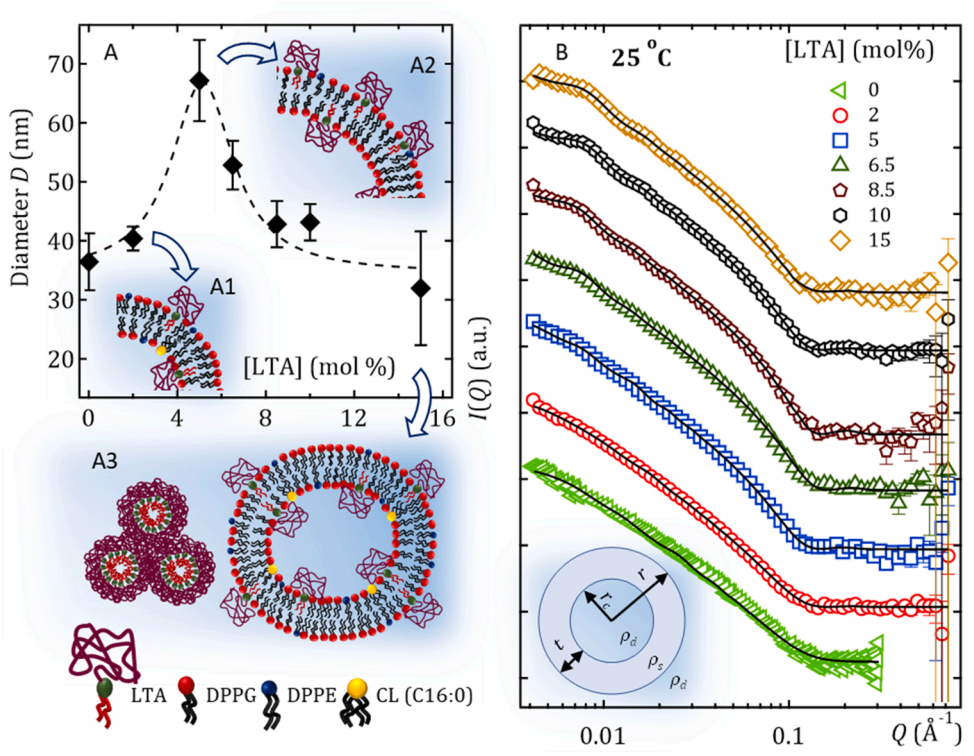

Fig. 2. (A) DLS number averaged diameter *D* of the mixed lipids vesicles as a function of LTA concentration at 25 °C. The dashed line is a guide to the eye. Schematic representation of the molecular packing of mixed vesicles at 25 °C: (*A1*) Mixed vesicles at low LTA concentration, (*A2*) increase in the vesicle size due to LTA-induced repulsion, and (*A3*) segregation of vesicles and LTA micelles at higher concentration with possible micelle clustering. (B) SANS intensity *I vs Q* profiles for liposomes containing 0 – 15 mol% LTA at 25 °C. Symbols are the data points and solid lines represent the best fits using the *spherical core-shell* model. For clarity, the SANS profiles are scaled on the *y*-axis. A mixed vesicle described by the *spherical core-shell model* with a core radius *rc* and an overall radius *r*. The shell thickness is thus $t = r - r_c$.

3. Results and discussion

3.1. Effect of LTA concentration on the mixed vesicle structure: DLS and SANS measurements

The size distribution of the mixed lipid vesicles was examined by dynamic light scattering (DLS) measurements as a function of LTA concentration at 25 °C. The number averaged diameter *D* for the mixed vesicles at different LTA concentrations (Fig. 2A) increased from 36.5 ± 4.8 nm to 67.1 ± 6.9 nm upon increasing the LTA concentration ([LTA]) up to 5 mol% and then decreased as more LTA was added. The large molecular volume of LTA compared to phospholipids and its highly negatively charged polyglycerolphosphate backbone are expected to alter molecular packing in the liposomes, thus causing structural changes driven by steric and electrostatic interactions. The *intensity* averaged DLS size distribution (cf. Figure S3 in SI), which is more sensitive to larger aggregates even present in trace amounts, shows the emergence to two peaks (i.e. two aggregate/liposome sizes). This points to the possible presence of liposome clusters in trace amounts.

LTA is present in relatively low molar concentrations (~ 6–12 mol% with respect to the total lipid content) in Gram-positive bacteria membranes. [11,18] Gutberlet et al. reported mixing of *Staphylococcus aureus* LTA up to 15 mol% concentration with DPPG [27] and DPPC [28] in an LB monolayer formed at the air-water interface; however, phase separation occurred on further LTA addition. The change in the mean molecular area and surface pressure values suggested that low concentrations of LTA (comparable to that present in actual bacteria membranes) could affect the stability and rigidity of the phospholipid membrane. The bulky LTA molecule and thus the resultant steric hindrance and the repulsion between the negative charges on the polyglycerolphosphate headgroup would favour an increase in the vesicle size. However, no clear explanation could be derived for the decrease in the vesicle size at higher LTA concentrations. The DLS results provided limited information about the structure and morphology of the aggregates, which was further probed using cryo-TEM and SANS measurements.

The absolute SANS intensity (Figure S4 in SI) increased with the LTA concentration up to 6.5 mol%. With further increase in the LTA concentration, the scattering intensity remained the same and the fringes at the lower *Q* region became more pronounced, indicating possible formation of large aggregates. The scattering intensity for the mixed vesicles containing 15 mol% LTA showed a similar profile as that for 2 mol% LTA.

The SANS profiles in the *Q* range of 0.0045 to 0.7 $Å^{-1}$ for the mixed vesicles in aqueous solutions in the presence of different LTA mol% at 25 °C are shown in Fig. 2B. The best-fit parameters using the *spherical*

Table 1
Fitted SANS parameters for the mixed vesicles as a function of LTA concentration ([LTA]) in mol% at 25 °C. Here *r* is the radius of vesicles, *t* the thickness of the vesicle shell, ϕ the volume fraction of the shell, PDI the polydispersity index from the SANS measurements for the measured *r* values, and χ^2 an indication of the goodness of the fit. The DLS radius (*D*/2) values are also included for comparison.

[LTA]	*r* (nm)	*D*/2 (nm) (from DLS)	*t* (nm)	ϕ	PDI (σ/r)	χ^2
0	19.5 ± 2.7	18.2 ± 2.4	2.9 ± 0.70	0.0035	0.34	0.5
2	21.3 ± 0.4	20.2 ± 1.0	3.9 ± 0.03	0.0022	0.33	2.3
5	35.8 ± 0.2	33.6 ± 3.4	4.3 ± 0.07	0.0025	0.29	4.0
6.5	36.3 ± 0.3	26.4 ± 2.1	4.0 ± 0.05	0.0032	0.36	14.1
8.5	36.1 ± 0.1	21.4 ± 2.0	4.2 ± 0.08	0.0026	0.40	2.1
10	31.8 ± 0.2	21.5 ± 1.5	4.2 ± 0.07	0.0028	0.43	2.0
15	27.3 ± 0.8	15.9 ± 4.8	3.8 ± 0.10	0.0029	0.62	3.1

core-shell model are listed in Table 1. Overall, the fitted vesicle size is comparable to that obtained from DLS (cf. Table 1). The fitting was also attempted using the *core-shell ellipsoid model* and the *Guinier-Porod analysis*, but no physically feasible parameters were achieved (cf. Section S1 in SI). The SANS profile for the ternary phospholipid composition (PG/PE/CL mixture; [LTA] =0 mol%) could be well fitted to the *spherical core-shell model* with a radius $r \sim 19$ nm and a shell thickness $t = 2.9$ nm. The addition of 2 mol% LTA increased the shell thickness to $t = 3.9$ nm, which indicates that the mixing of LTA with the lipids induced structural changes to the shell. With further increase in the LTA concentration to 6.5 mol%, the average radius of the mixed vesicles increased to $r \sim 36$ nm, indicating further incorporation of LTA in the shell. The observed increase in the radius and the thickening of the shell could be correlated with the enhanced steric hinderance due to the incorporation of the bulky LTA molecules and the increased electrostatic repulsion between negatively charged LTA phosphate groups and the phospholipids.

The PDI values for [LTA] > 8.5 mol% indicate significant variation in the distribution of the vesicle radius, and a decrease in the radius for the mixed vesicles for [LTA] = 10 and 15 mol% indicates a possible segregation of the formed structures. The vesicle radius decreased to $r \sim 27$ nm, while the shell thickness $t \sim 3.8$ nm for [LTA] =15 mol%. The double distribution obtained for intensity average DLS data (cf. Figure S3 in SI) in the presence of 15 mol% LTA indicates the presence of aggregates of different sizes, possibly due to preferred LTA micellization over mixed vesicle formation and clustering of some liposomes. The observed increase in the PDI values with LTA addition is consistent with the Cryo-TEM images showing formation of large vesicles along with the interconnected small vesicles (cf. Fig. 3 below). This is also largely comparable with the PDI values measured by the DLS between 0.4−0.6 (cf. Table S3 in SI).

The strong electrostatic repulsive forces between LTA polyphosphates may constrain LTA crowding and its further incorporation and mixing with the phospholipids in the membrane as more LTA was added. The liposome size reduction was accompanied by concurrent membrane thinning, consistent with reduced elastic bending energy cost. This observation is in agreement with the previous reports by Gutberlet et al. [27,28] that showed mixing of LTA with phospholipids at very low concentrations and subsequent stabilization of the monolayers at the air-water interface. Our SANS results seem to suggest that LTA could stabilise the membrane structures up to a certain LTA concentration (~6.5 mol%). This is comparable to the LTA concentration in the bacteria membrane at ~ 6−12 mol%. The change in vesicle structure with LTA incorporation is schematically illustrated in Fig. 2A1−3), which indicates an increase in the size of aggregates due to an increase in the area occupied by the molecules.

The LTA molecules are presumably incorporated in the lipid bilayer through the hydrophobic interaction, occupying a larger mean molecular area and causing stronger repulsion due to the bulky and charged glycerolphosphate chains. It is conceivable that LTA molecules could be incorporated in both the inner and outer leaflet of the liposome bilayer (cf. Fig. 2A1−3)). The decrease in the vesicles radius r at higher concentration may be rationalised with three considerations. First, at higher LTA concentrations (> 8.5 mol%), an increase in the mean molecular area occupied by the constituent molecules may lead to a critical threshold, which prevented further LTA incorporation. Secondly,

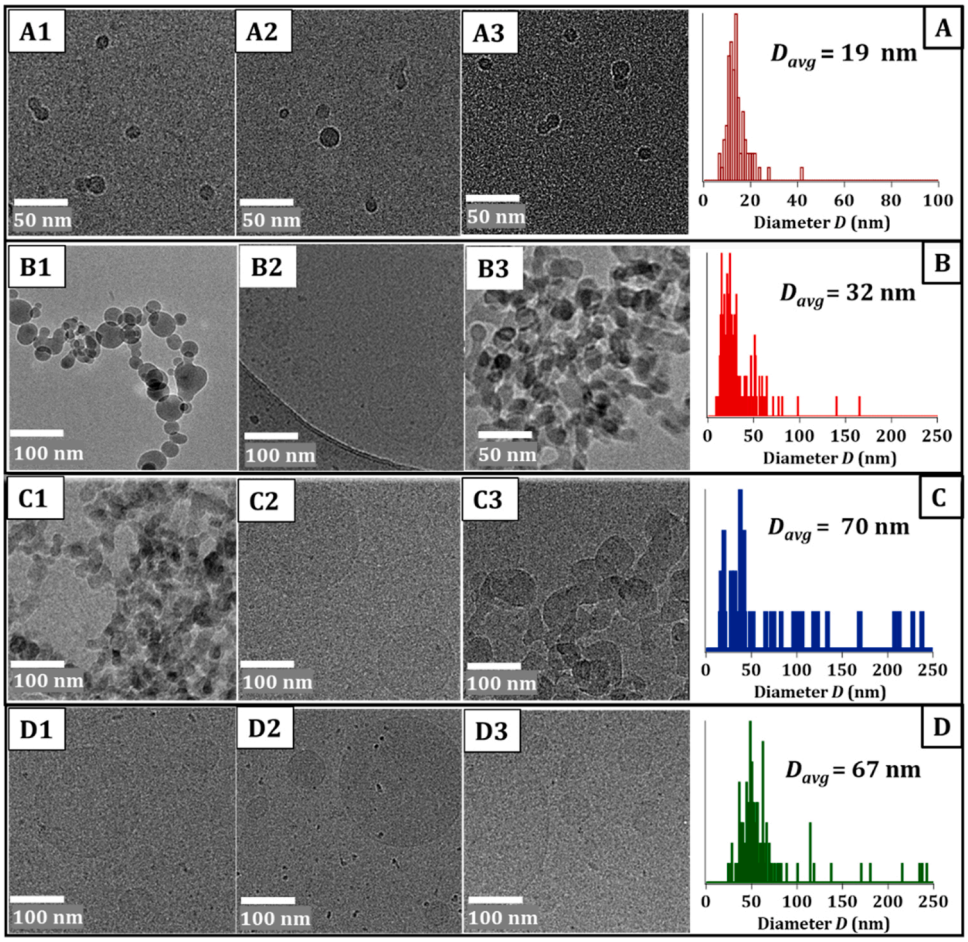

Fig. 3. Cryo-TEM images of vesicles (1 mg mL^{-1}) in aqueous solution in the presence of different LTA concentration: (A) 0 mol%, (B) 2 mol%, (C) 5 mol%, and (D) 10 mol%. Three different images are presented along with and the histograms for the average diameter D_{avg}.

further LTA addition might favour a higher number of smaller vesicles in which a smaller number of LTA molecules could be incorporated to minimise inter-LTA repulsion. Alternatively, LTA micelles might compete with the mixed vesicles for LTA molecules. Thirdly, during the preparation of the vesicle dispersion, the lipid film was hydrated with aqueous LTA solution, which contained LTA micelles in dynamic equilibrium with monomers. The mixing of LTA with lipids became less efficient with an increase in the micelle number density at the higher LTA concentrations.

3.2. Morphology of mixed liposomes by Cryo-TEM

The size and morphology of the mixed vesicles were visualised using Cryo-TEM as shown in Fig. 3. In the absence of LTA, the spherical vesicles were evident with an average diameter $D \sim 19$ nm. With 2 mol% LTA added (cf. Fig. 3B1−3)), D increased to ~ 32 nm, suggesting that LTA induced an increase in the mean molecular area in the mixed vesicles, with large structures of size in excess of 100 nm also present. The morphology of the mixed vesicles remained largely spherical with some interlinking among smaller aggregates. This could be attributed to hydrogen bonding between the −OH groups of the glycerolphosphate units of the LTA molecules between adjacent vesicles.

For 5 mol% LTA mixed vesicles (cf. Fig. 3C1−3)), clusters of small aggregates and the presence of large vesicles were observed with an average size $D \sim 70$ nm. This is consistent with the high PDI observed in the SANS experiment (shown later). The average diameter for 10 mol% LTA containing vesicles was $D \sim 67$ nm (cf. Fig. 3D1−3)), but the number density of larger vesicles increased as compared to 5 mol% LTA. The number of clustered smaller structures decreased compared to lower LTA concentrations, which indicates a possible decrease in the mixing of LTA with lipids present in the vesicles, with the excess LTA molecules aggregating to form micelles. The negative stain TEM images on pure LTA micelles, vesicles excluding LTA and vesicles in the presence of 5 mol% LTA are shown in Figure S5 in SI. The observed morphology of the vesicles was in good agreement with the cryo-TEM images showing formation of spherical structures and an increase in the vesicle size with LTA addition.

3.3. Effect of temperature on the mixed vesicle structure: SANS measurements

The LTA polyglycerophosphate chains containing −OH groups may induce the formation of intermolecular and intramolecular H-bonding among them in the mixed vesicles and with the water molecules. In addition to the −OH groups, the D-alanine substituted structures in the LTA chain are also expected to engage in H-bonding. The SANS experiments were also performed at 45 and 80 °C to examine the temperate effects on the H-bonding tendencies and lipid chain fluidity. Higher thermal energy and chain melting are expected to influence the molecular packing of phospholipids and LTA molecules in the bilayer. The fluid phase transition temperature of DPPG (the major lipid molecule present in *Bacillus Subtilis* membrane) is $T_m \sim 41$ °C, which has been reported to shift to a higher value when mixed with LTA [18]. In the present investigation, the chain melting temperature for the quaternary lipid mixture comprising DPPG as major constituent (~70 mol%) in the presence of DPPE, cardiolipin and LTA is also expected to be higher as compared to pure DPPG.

The measured SANS profiles at 45 °C (Fig. 4A) show no significant variations in comparison to those at 25 °C (cf. Fig. 2B). The bilayer thickness remained constant at $t \sim 4$ nm and the vesicles radius increased from $r = 35.8$ nm to $r = 39.4$ nm as the LTA concentration increased from 2 to 5 mol%. However, no significant changes were noticed for higher [LTA]. The fitted radius r and shell thickness t for the vesicles at [LTA] = 0–15 mol% at different temperatures are shown in Fig. 5A and B, respectively. If the fluid phase transition temperature was shifted above 45 °C for LTA concentrations higher than 5 mol%, it is then conceivable that similar structural parameters for the mixed vesicles were observed compared to 25 °C. In addition to the electrostatic repulsion and the higher steric footprint of LTA, the vesicle size may be further influenced by the increase in the chain fluidity at elevated temperature.

With further increase in the temperature to 80 °C (Fig. 4B), the scattering profile showed an increase in slope in the low-Q region, accompanied by the diminishment of the fringes. The observed trend for the change in the absolute scattering intensity with the LTA addition remained consistent with that at lower temperatures (cf. Figure S4 in SI).

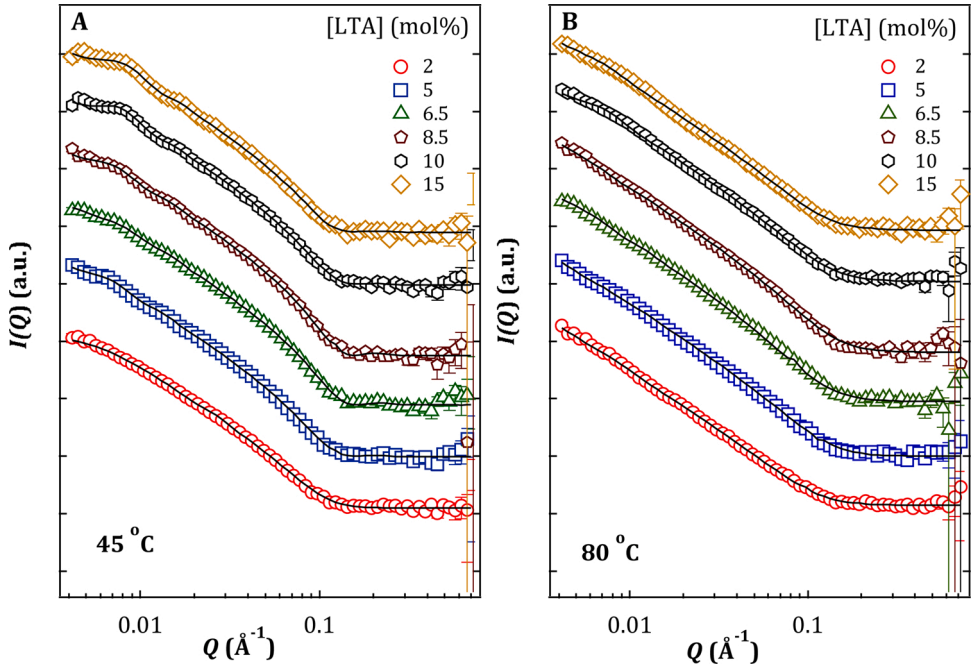

Fig. 4. SANS profiles for liposomes containing 0 – 15 mol% LTA at 45 °C (A) and 80 °C (B). Different symbols are the experimental data points and the solid lines represent the best fits using the *spherical core-shell model*. For clarity, the SANS profiles are scaled on the *y*-axis.

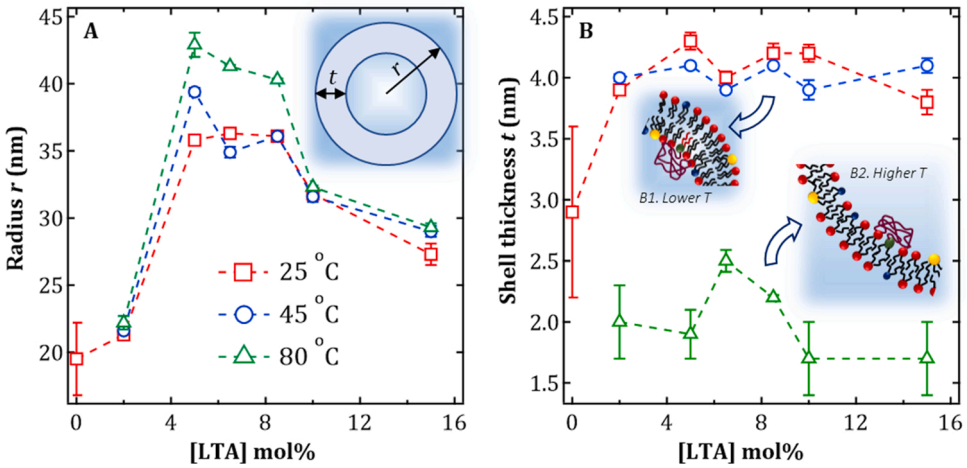

Fig. 5. The fitted radius *r* (A) and the shell thickness *t* (B) as a function of [LTA] in the mixed vesicles (inset) at 25, 45, and 80 °C. Schematic representation of molecular packing inside mixed vesicles containing LTA at lower temperatures (*B1*) and the higher temperature (*B2*).

As shown in Table S4, at 80 °C the vesicle radius increased from $r \sim 22$ nm to $r \sim 43$ nm as [LTA] increased from 2 to 5 mol%. This was accompanied by a decrease in the bilayer thickness from $t \sim 4.0$ nm to $t \sim 1.9$ nm, indicating a significant increase in the chain fluidity and subsequent thinning of the shell due to chain interdigitation. The PDI increased with the LTA addition suggesting considerable change in the size distribution as a function of LTA at 80 °C. The PDI value increased to 0.69 in the presence of 15 mol% LTA from an initial value of 0.34 measured for the 2 mol% LTA containing vesicles.

At temperatures below the fluid phase transition temperature, the saturated (C16:0) lipid chains are expected to pack tightly in the bilayer, which is reflected in the higher values of the bilayer thickness *t* at 25 and 45 °C compared to 80 °C. It has been previously suggested that the sodium counterions of DPPG and DPPE are distributed further away from the vesicle surface at elevated temperatures due to their increased kinetic energy, which would result in weaker screening of electrostatic charges and higher repulsion between lipids [29]. The decrease in the bilayer thickness *t* at 80 °C is associated with an increase in the lipid chain entropy, which results in the broadening of the molecular conformation and an increase in the headgroup area [30]. The extent of H-bonding between water and the −OH groups present in the polyglycerolphosphate chain of LTA is expected to decrease at higher temperatures. As a result, the in-plane electrostatic repulsion between the LTA phosphate groups and the phospholipids would increase due to more compact polyglycerolphosphate chains. On the other hand, the increased fluidity of lipid chains would increase the area occupied by LTA molecules at higher temperatures, leading to the conformational changes of the lipid chains that favour the thinning of the membrane with an increase in the temperature. These combined effects would lead to an increase in the area occupied by the lipid and LTA molecules, accompanied by an increase in the vesicle size. The possible arrangement of constituent molecules in the vesicles at 80 °C is schematically represented in Figure 5B2.

Our observations are consistent with several previous reports on temperature induced structural changes in the vesicle size [30,31]. SAXS revealed an increase in the mixed DOPS/DLPS vesicle size accompanied by a decrease in the bilayer thickness [30]. These changes were attributed to weaker electrostatic screening by the counterions at higher temperatures and increased lipid chain entropy. A SANS study on phospholipid ULVs revealed similar effects of temperature on the aggregate structure [31]. In the current investigation, DPPE and cardiolipin (minor phospholipid components in the *Bacillus Subtilis* membrane) may facilitate an increase in the vesicle size to a certain extent, driven by the fluidization of the membrane. The headgroup of DPPE (cf. Figure 1B2) is considerably smaller compared to PG and cardiolipin, whilst cardiolipin with four hydrocarbon chains and a larger headgroup (cf. Figure 1B4) compared to PG and PE may occupy a larger molecular area, both helping to balance the molecular packing in the vesicle.

To examine the reversibility of temperature-induced structural changes, SANS was performed as the samples were cooled back to 25 °C. The SANS profiles are very similar to those collected before heating (cf. Fig. 2B), as shown in Figure S6. The fitted values of the vesicle shell thickness *t* were smaller, while the radius *r* values were similar, compared to the initial 25 °C data before heating (Table S4). In the presence of 5 mol% LTA, the shell thickness $t \sim 3.3$ nm was lower than $t \sim 4.3$ nm observed at 25 °C before heating. *t* was further reduced to ~ 3 nm in the case of higher LTA concentration. However, an increase in the shell thickness compared to 80 °C can be attributed to the reduced chain fluidity, which led to closer packing in the shell.

A previous SANS study [32] showed that mixed PC/PG bicelles formed at 45 °C, which transformed to monodisperse core-shell oblate ellipsoids upon cooling to 10 °C. It was also reported that the radius of Ca^{2+}-doped DMPC ULVs decreased by 50 Å upon cooling to 10 °C from initial 45 °C [33]. Liu et al. reported transformation of DMPC/DHPC/DMPG mixed spherical vesicles at 50 °C to an oblate shape upon cooling to 10 °C by fitting the SANS data using an oblate single shell model [34]. In the present investigation, the structural changes in the vesicles at the higher temperature were not completely reversible upon cooling, but the spherical shape was retained at all the temperatures. The observed higher *r* values compared to the cryo-TEM is understandable, as SANS provides an averaged sizing over a much larger sample volume, whereas cryo-TEM provides the local information on selected region of the sample.

4. Conclusion

Mixed liposomes mimicking the composition of the Gram-negative bacterial membrane, comprising DPPG/DPPE/CL(C16:0) phospholipid mixtures and incorporating *Bacillus Subtilis* LTA, have been investigated using DLS, cryo-TEM, and SANS to understand the effect of LTA concentration (in the range 0–15 mol%) on the structure of the mixed vesicles. The DLS results indicate that LTA induced an increase in the size of the mixed vesicles up to ~6.5 mol%. Cryo-TEM and negative stain images indicated formation of spherical shape vesicles that increased in the average diameter *D* with LTA addition. The presence of large vesicles and interconnected small vesicles are indicative of polydisperse distribution of LTA mixed vesicles. Similarly, SANS data analysis revealed an increase in the radius *r* of spherical vesicles on addition of LTA up to 6.5 mol%, which is attributed to steric and electrostatic interactions among the constituent molecules in the mixed membrane due to LTA

incorporation. Upon further LTA addition, the vesicle size decreased due to competitive LTA micelle formation or partition of LTA into smaller vesicles to address the unfavourable repulsions due to LTA. This observed non-monotonic vesicle-size variation with respect to LTA concentration - increasing up to LTA concentration ~ 6.5 mol% - can be correlated with the LTA concentrations found in the real bacteria membrane (*i.e.* 6−12 mol% depending on bacteria species [11,18]). This threshold is interpreted as being due to LTA preferential self-aggregation at higher concentrations to satisfy optimal intermolecular forces and molecular packing of LTA and other lipids in the mixed membrane, which limits further incorporation of LTA molecules in the bilayer at higher concentrations. In future experiments, this hypothesis could be further tested by e.g. adding LTA to pre-formed vesicles at the LTA concentration close to this threshold to check if they would be transformed into the smaller variant. This dynamic process would involve membrane reconfiguration *via* destabilization, bilayer disassembly, and then re-nucleation of new vesicles in solution, which is of interest for further investigations.

No significant changes in the aggregation behaviour were noticed with the increase in temperature to 45 °C, and this could be rationalised by the elevated chain melting temperature of the lipid mixtures compared to the pure bilayer. An increase in the vesicle size and thinning of the vesicle shell was observed at 80 °C. This could be attributed to an increase in the lipid chain entropy and broader diffusion of the counterions away from the headgroups. Cooling of vesicles to 25 °C resulted in partial recovery of formed structures with vesicles equilibrating close to the initial size, while the shell was thinner than the initial value at 25 °C before heating. These unprecedented experimental observations shed light on the intermolecular interactions between LTA and bacterial membrane lipids and the effects of such interactions on the membrane structure.

CRediT authorship contribution statement

Bhavesh Bharatiya: Investigation, Methodology, Validation, Formal analysis, Data curation, Writing - original draft. **Gang Wang:** Methodology, Data curation. **Sarah E. Rogers:** Data curation, Resources. **Jan Skov Pedersen:** Validation, Data curation. **Stephen Mann:** Validation, Writing - review & editing. **Wuge H. Briscoe:** Conceptualization, Resources, Supervision, Writing - review & editing, Project administration.

Declaration of Competing Interest

The authors declare that they have no known competing financial interests or personal relationships that could have appeared to influence the work reported in this paper.

Acknowledgement

We acknowledge the ISIS Muon and Neutron Source for the awarded beamtime under experiment number RB-1920280 and thank Lauren Matthews, Charlotte Kenton, and Nick Taylor for their help with the SANS measurements. We also acknowledge the Wolfson Foundation for establishing the Wolfson Bioimaging Facility, University of Bristol. We would like to acknowledge Dr Judith Mantell for her help with use of the microscopes in the Wolfson Bioimaging Facility. BB is supported by a Marie Sklodowska- Curie actions for the funding (Proposal No: 797038).

Appendix A. Supplementary data

Supplementary material related to this article can be found, in the online version, at doi:https://doi.org/10.1016/j.colsurfb.2020.111551.

References

[1] I. Ginsburg, Role of lipoteichoic acid in infection and inflammation, Lancet Infect. Dis. 2 (3) (2002) 171–179.
[2] A. Tripathy, P. Sen, B. Su, W.H. Briscoe, Natural and bioinspired nanostructured bactericidal surfaces, Adv. Colloid Interface Sci. 248 (2017) 85–104.
[3] C. Redeker, W.H. Briscoe, Interactions between mutant bacterial lipopolysaccharide (LPS-Ra) surface layers: surface vesicles, membrane fusion, and effect of Ca2+and temperature, Langmuir 35 (48) (2019) 15739–15750.
[4] R. Amils, Gram-positive bacteria, in: M. Gargaud, R. Amils, J.C. Quintanilla, H. J. Cleaves, W.M. Irvine, D.L. Pinti, M. Viso (Eds.), Encyclopedia of Astrobiology, Springer Berlin Heidelberg, Berlin, Heidelberg, 2011 pp 685-685.
[5] V.A. Fischetti, R.P. Novick, J.J. Ferretti, D.A. Portnoy, M. Braunstein, J.I. Rood, Gram-Positive Pathogens, Vol. 29, John Wiley & Sons, 2019.
[6] G. Seltmann, O. Holst, The Bacterial Cell Wall, Springer Science & Business Media, 2013.
[7] E. Huff, Lipoteichoic acid, a major amphiphile of Gram-positive bacteria that is not readily extractable, J. Bacteriol. 149 (1) (1982) 399.
[8] M.P. Glauser, Pathophysiologic basis of sepsis: considerations for future strategies of intervention, Crit. Care Med. 28 (9 Suppl) (2000) S4–S8.
[9] V.R. Matias, T.J. Beveridge, Lipoteichoic acid is a major component of the Bacillus subtilis periplasm, J. Bacteriol. 190 (22) (2008) 7414–7418.
[10] S. Clejan, T. Krulwich, K. Mondrus, D. Seto-Young, Membrane lipid composition of obligately and facultatively alkalophilic strains of Bacillus spp, J. Bacteriol. 168 (1) (1986) 334–340.
[11] W. Fischer, Lipoteichoic acid and lipids in the membrane of *Staphylococcus aureus*, Med. Microbiol. Immunol. 183 (2) (1994) 61–76.
[12] F. Prossnigg, A. Hickel, G. Pabst, K. Lohner, Packing behaviour of two predominant anionic phospholipids of bacterial cytoplasmic membranes, Biophys. Chem. 150 (1–3) (2010) 129–135.
[13] Á. Oszlánczi, A. Bóta, E. Klumpp, Influence of aminoglycoside antibiotics on the thermal behaviour and structural features of DPPE–DPPG model membranes, Colloids Surf. B Biointerfaces 75 (1) (2010) 141–148.
[14] Á. Oszlánczi, A. Bóta, E. Klumpp, Layer formations in the bacteria membrane mimetic DPPE-DPPG/water system induced by sulfadiazine, Biophys. Chem. 125 (2–3) (2007) 334–340.
[15] Á Oszlánczi, A. Bóta, S. Berényi, E. Klumpp, Structural and morphological changes in bacteria-membrane mimetic DPPE/DPPG/water systems induced by sulfadiazine, Colloids Surf. B Biointerfaces 76 (2) (2010) 519–528.
[16] A. Arouri, M. Dathe, A. Blume, Peptide induced demixing in PG/PE lipid mixtures: a mechanism for the specificity of antimicrobial peptides towards bacterial membranes? Biochim. Biophys. Acta 1788 (3) (2009) 650–659.
[17] S. Danner, G. Pabst, K. Lohner, A. Hickel, Structure and thermotropic behavior of the Staphylococcus aureus lipid lysyl-dipalmitoylphosphatidylglycerol, Biophys. J. 94 (6) (2008) 2150–2159.
[18] T. Gutberlet, J. Frank, H. Bradaczek, W. Fischer, Effect of lipoteichoic acid on thermotropic membrane properties, J. Bacteriol. 179 (9) (1997) 2879–2883.
[19] http://www.isis.stfc.ac.uk (accessed: October 2019) ISIS Science & Technology Facilities Council, 2019.
[20] R. Heenan, S. Rogers, D. Turner, A. Terry, J. Treadgold, S. King, Small angle neutron scattering using Sans2d, Neutron News 22 (2) (2011) 19–21.
[21] Mantid Project, http://www.mantidproject.org (accessed: October 2019).
[22] B.J. Berne, R. Pecora, Dynamic Light Scattering: With Applications to Chemistry, Biology, and Physics, Courier Corporation, 2000.
[23] A. Guinier, G. Fournet, K.L. Yudowitch, Small-angle Scattering of X-rays, 1955.
[24] M. Kotlarchyk, S.H. Chen, Analysis of small angle neutron scattering spectra from polydisperse interacting colloids, J. Chem. Phys. 79 (5) (1983) 2461–2469.
[25] J.K. Percus, G.J. Yevick, Analysis of classical statistical mechanics by means of collective coordinates, Phys. Rev. 110 (1) (1958) 1.
[26] S. Morath, A. Geyer, I. Spreitzer, C. Hermann, T. Hartung, Structural decomposition and heterogeneity of commercial lipoteichoic acid preparations, Infect. Immun. 70 (2) (2002) 938–944.
[27] T. Gutberlet, S. Markwitz, H. Labischinski, H. Bradaczek, Monolayer investigations on the bacterial amphiphile lipoteichoic acid and on lipoteichoic acid/dipalmitoylphosphatidylglycerol mixtures, in: Makromolekulare Chemie. Macromolecular Symposia, Wiley Online Library, 1991, pp. 283–287.
[28] T. Gutberlet, K. Milde, H. Bradaczek, H. Haas, H. Möhwald, Miscibility of lipoteichoic acid in dipalmitoylphosphatidylcholine studied by monofilm investigations and fluorescence microscopy, Chem. Phys. Lipids 69 (2) (1994) 151–159.

[29] D. Andelman, Electrostatic properties of membranes: the Poisson-boltzmann theory, in: Handbook of Biological Physics, Vol. 1, Elsevier, 1995, pp. 603–642.
[30] P. Szekely, T. Dvir, R. Asor, R. Resh, A. Steiner, O. Szekely, A. Ginsburg, J. Mosenkis, V. Guralnick, Y. Dan, Effect of temperature on the structure of charged membranes, J. Phys. Chem. B 115 (49) (2011) 14501–14506.
[31] J. Pencer, T. Mills, V. Anghel, S. Krueger, R.M. Epand, J. Katsaras, Detection of submicron-sized raft-like domains in membranes by small-angle neutron scattering, Eur. Phys. J. E 18 (4) (2005) 447–458.
[32] M.-P. Nieh, V.A. Raghunathan, S.R. Kline, T.A. Harroun, C.-Y. Huang, J. Pencer, J. Katsaras, Spontaneously formed unilamellar vesicles with path-dependent size distribution, Langmuir 21 (15) (2005) 6656–6661.
[33] M.-P. Nieh, T. Harroun, V. Raghunathan, C. Glinka, J. Katsaras, Concentration-independent spontaneously forming biomimetric vesicles, Phys. Rev. Lett. 91 (15) (2003), 158105.
[34] Y. Liu, M. Li, Y. Yang, Y. Xia, M.-P. Nieh, The effects of temperature, salinity, concentration and PEGylated lipid on the spontaneous nanostructures of bicellar mixtures, Biochimica et Biophysica Acta (BBA)-Biomembranes 1838 (7) (2014) 1871–1880.